

Elastic Flattening of Painted Pottery Surfaces

Reinhold Preiner¹ Stephan Karl² Paul Bayer² Tobias Schreck¹

¹Graz University of Technology, Institute of Computer Graphics and Knowledge Visualization, Austria

²University of Graz, Department of Archaeology, Austria

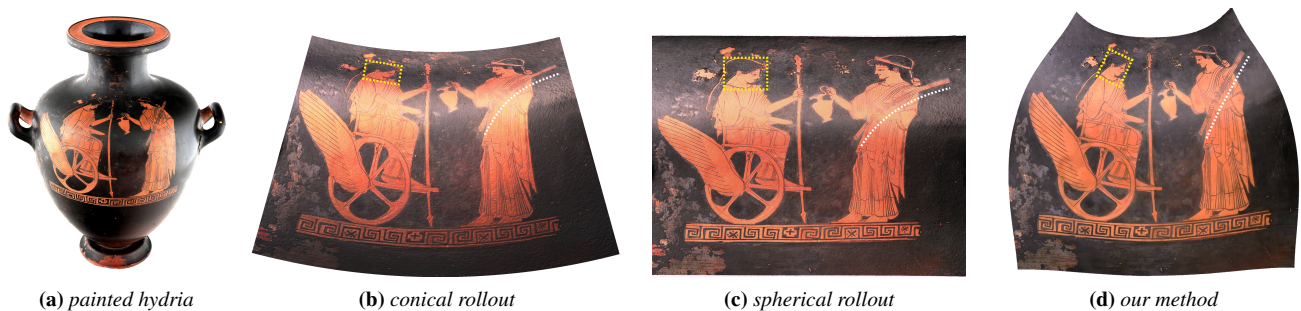


Figure 1: Capturing the texture of a bulgy hydria (a). Current methods rely on rollouts of proxy geometries like cones (b) or spheres (c) onto which the surface is projected. These often result in strong anisotropic distortions (dotted box and line), making them unsuitable for archaeological use cases like documentation or classification. Our method globally minimizes edge distortions of a flattened surface mesh using an elastic spring model, thereby much better preserving local image proportions crucial for a faithful assessment of a painting (d).

Abstract

Generating flat images from paintings on curved surfaces is an important task in Archaeological analysis of ancient pottery. It allows comparing styles and painting techniques, e.g. for style and workshop attribution, and serves as basis for domain publications which typically use 2d images. To obtain such flat images from scanned textured 3d models of the pottery objects, current practice is to perform so-called rollouts using approximating shape primitives like cones or spheres, onto which the mesh surfaces are projected. While this process provides an intuitive deformation metaphor for the users, it naturally introduces unwanted distortions in the mapping of the surface, especially for vessels with high-curvature profiles. In this work, we perform an elastic flattening of these projected meshes, where stretch energy is minimized by simulating a physical relaxation process on a damped elastic spring model. We propose an intuitive contraction-directed physical setup which allows for an efficient relaxation while ensuring a controlled convergence. Our work has shown to produce images of significantly improved suitability for domain experts' tasks like interpretation, documentation and attribution of ancient pottery.

CCS Concepts

•Computing methodologies → Physical simulation; Optimization algorithms; Texturing;

1. Introduction

The drawing of pottery paintings in the form of a rollout is an essential element of the object documentation in archaeological pottery research. It has a long tradition in classical archaeology, especially in the study of Greek vases [Wal08]. By means of these scientific drawings the decoration is set entirely free from the pottery shape, allowing to capture the paintings on curved surfaces without photographic distortion, or as a whole in cases of circumferential paintings. These drawings support the determination of characteris-

tics of a painter and facilitate the stylistic comparison and connection between figures or ornaments on different objects. To this day, works in classical archaeology have sufficiently demonstrated the importance of drawings for elaborating a classification of individual artists and workshops [Sch, Gra14]. Creating an accurate drawing of a painted surface, however, is tricky and time-consuming. First approaches relied on manually tracing off these drawings using tracing paper with direct contact on the curved pottery surface, and then redrawing them in a final version [Ric36]. Besides being

tedious and not contact-free, this approach often introduces indeterministic distortions of distance relations due to the copyist's continuous manual adjustment of the tracing paper on those painted surface parts. To overcome these problems and to accelerate the documentation tasks in pottery studies, 3D acquisition and the application of computer-aided reconstruction and geometric processing methods have gained increasing importance. Based on a 3d mesh representation, various software tools allow performing virtual rollouts in a standardized and reproducible way. The most comprehensive technique currently used by archaeologists projects the texture of the pottery surfaces onto proxy surfaces of revolution like conical frustums (Fig. 1b), or spheres and spherical segments (Fig. 1c). While this method of unrolling works sufficiently well for objects that can be well approximated by these proxy surfaces, it is of limited use for highly curved shape profiles, as commonly present in Greek pottery [Sch99] (see Fig. 1a). In these cases, such rollouts typically cause significant distortions, hindering a realistic impression and an accurate archaeological investigation of its painting.

Instead of a projection-based rollout, we propose to use a physical based flattening approach that globally minimizes surface distortions in the projected or unrolled surfaces. Our method performs a physical relaxation simulation using an elastic spring system which is defined on the flattened input mesh and encodes distortion in spring potential energy. We propose an intuitive physical setup that directs the relaxation towards a controlled contraction, thus allowing for an efficient relaxation while ensuring stable convergence. This way, local surface distortions are evenly distributed over the flattened mesh, keeping local proportions of painted subjects mainly intact (see Fig. 1d). Our method faithfully captures paintings of interest for the archaeologists on ancient Greek vessels with strongly curved surface profiles, for which currently used rollout methods have not been able to produce satisfactory results.

2. Related Work

Generating a flat image of the surface of an arbitrary 3d object is generally a *mapping* problem, or similarly, finding a suitable *surface parametrization* of a given 3d shape. It is well known that any parametrization of a non-developable 3d surface necessarily results in distortions in the mapped image, which are hardly comprehensible by inspecting the final image alone. For the analysis, classification and comparison work of painted pottery, it is however important for archaeologists to intuitively understand how the flattened image was produced and where distortions are present. Current practice is to apply an unrolling of proxy surfaces of revolution fitted to a digitized mesh model, which provides an intuitive physical metaphor. One of the tools most widely used by archaeologists for creating these so-called *rollouts* is the *GigaMesh* software framework [BKMK10, MP13].

For nearly *spherical* shapes unwrapping the surface in form of a rollout typically introduces significant distortions if paintings cover regions close to the poles, as shown in Fig. 1. For spherical shapes like the earth, this problem is most prominently studied in cartography [Mac04]. Various approaches exist for projection of the earth surface to flat maps, e.g., conformal techniques preserving angles, techniques for preserving areas or distances, or directions from a central point. Another approach is to combine local projections in

a non-continuous way using cuts, trading mapping continuity for angle and distance preservation [VW08]. In general, no projection technique preserves all of the desired properties simultaneously, hence the choice is typically depending on the user task.

Surface parametrizations of *arbitrary* 3d shapes were intensively studied in computer graphics for tasks like texture mapping, geometric modelling and processing. A comprehensive survey of techniques and their applications was given by Floater and Hormann [FH05] and Sheffer et al. [SPR06]. A particular group of methods follow the approach of actually *flattening* a 3d input mesh. McCartney et al. [MCC99] proposed an sequential triangle insertion and subsequent energy relaxation. Sheffer et al. formulated the flattening problem as a constrained nonlinear optimization based on the angles of the mesh faces [SdS01, SLMB05]. Zayer et al. proposed a linear variant [ZLS07]. Liu et al. [LZX*08] combined a local flattening of each individual triangle with a global stitch operation for the entire mesh. A more intuitive shape deformation metaphor is given by *physical elasticity models*, which minimize distortions via a physical relaxation process of an elastic material modelled as a mass-spring system. These methods require specific care in order to avoid self collisions, which typically cause unwanted surface foldings in the planar case. Wang et al. [WAN02] considers mass and stiffness properties, and uses a penalty force repelling a vertex from its one-ring edges. Li et al. [LZL*05] inserted additional cross springs across winged triangle pairs to increase stability and avoid overlaps. Wang et al. [WAN05] minimizes deformation energy using a fitted woven mesh model, which resamples the input mesh to a regular grid of springs. Zong et al. [ZHO06] used additional bending forces for opening each winged triangle pair of a 3d mesh, followed by forcing and colliding the mesh to a plane. Chen et al. [CWB11] proposed a linear-elastic finite element method, iteratively striving for an equilibrium of internal physical forces, reporting fast results on smaller models. Yi et al. [YYZ*18] recently used a physical shell model incorporating hinge-based energies to unbend winged triangles, forcing a 3d mesh towards a plane. The results however depend on carefully balancing stiffness and hinge bending forces. Most of these methods were applied to small or moderately sized meshes, or were designed for specific applications like cloth modelling in garment design.

For flattening 3d models of ancient pottery, we are mostly dealing with large meshes representing surfaces of revolution, for which a suitable starting point for relaxation is already given by simple rollouts. This simplifies the relaxation problem to the two-dimensional domain, omitting e.g. the need to consider hinge bending forces. We use a robust physical based mass-spring implementation to flatten high-resolution meshes of digitized pottery to faithfully capture their texture. Our method employs an intuitive relaxation metaphor, which avoids overlaps in a more controllable way via a specific utilization of friction forces.

3. Elastic Relaxation

Our approach starts with an initial projection of a mesh to the 2d plane, either based on a given planar rollout or a simple orthogonal projection for paintings covering a smaller angle of revolution. In any case, our method aims at minimizing visible surface distortions produced by these simple projections. Let M be the original 3d

mesh with vertices $v_i \in V$ and M' its initial projection with points $x_i \in X$ on the plane. Local surface distortion in M' is measured via the stretch of its edges (i, j) with respect to their original length $r_{ij} = \|v_i - v_j\|$ in M . The global objective function to be minimized is given by the elastic potential energy

$$E(S_M) = \frac{1}{2} \sum_i^N \sum_{j \in \mathcal{N}_i} k (\|x_i - x_j\| - r_{ij})^2 \quad (1)$$

of a corresponding elastic spring system S_M defined over M' by employing its edges as springs. Here, \mathcal{N}_i denotes the set of neighbors connected to vertex i via a spring, k defines the spring stiffness, and r_{ij} the rest lengths the springs strive to restore via relaxation. Relaxation is performed via a physical simulation that optimizes the flattened vertex positions X with respect to minimizing Eq. (1). Its negative gradient defines the total Hookean restoring force

$$F_s(i) = - \sum_{j \in \mathcal{N}_i} k (\|x_i - x_j\| - r_{ij}) \frac{x_i - x_j}{\|x_i - x_j\|} \quad (2)$$

for each vertex i , which drives the relaxation. Vertex movement is then achieved via numerical integration of the equations of motion.

4. Physical Convergence Control

Directly using Eq. 2 as position update vector of a vertex equals to an ordinary gradient descent, naturally converging very slowly. The decisive benefit of a physical simulation is the preservation of momentum, which allows for continuous acceleration and thus a faster convergence. However, if the current momentum outweighs a currently opposing spring force, triangle collisions will occur, often resulting in unwanted overlaps which the residual strain energy might not be able to resolve. To counter this problem, one can use penalty forces repelling a vertex from its one ring edges [WAN02] or additional springs to vertices across those edges to keep them at distance [LZL*05]. These measures improve stability, but cannot guarantee to avoid overlaps, if the potential energy from the initial distortion results in too large opposing momentums. Another approach is to expose vertices under motion to friction, resulting in a damped spring system. However, too strong damping again results in a slow, momentum agnostic motion like gradient descent, and in general, globally uniform damping is not guaranteed to prevent acceleration variances resulting in collisions.

Our key insight is that collisions always follow a critical squeezing of neighboring mesh regions that strive for expansion. We thus use an intuitive physical setup to allow for a robust convergence control. First, we uniformly scale up the initial projected flat mesh by a certain factor to initially introduce a global stretch and relax initially squeezed regions that could result in opposing motion of expansion. This initial stretch forces the subsequent relaxation process to be dominated by a global contraction motion. This contraction turns out to be much more controllable when introducing a particular distribution of a frictional force $F_f(i) = -v_i \cdot c_i$ across the mesh, where v_i is current velocity of vertex i , and c_i its damping coefficient. To execute the contraction process in a controlled way, we apply a low friction ($c_i = 0.01$) to the interior mesh vertices driving the contraction, while using a large, critical friction ($c_i = 1$) for its boundary vertices, opposing the contractive motion and thus resulting in a fast but still robust convergence. Figure 2a

shows that areal expansion forces in the upper squeezed part of an initially projected mesh results in surface foldings, appearing as yellow wrinkles in the overlaid stress map. After stretching the mesh, collisions occur due to contraction (Fig. 2b). Using damping forces on the boundary allows for a robust contraction (Fig. 2c).

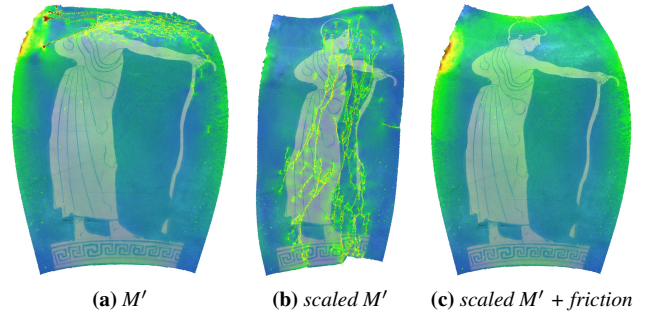


Figure 2: Robustness of elastic relaxation (a) on the initial projected mesh M' (b) after scaling M' by a stretch factor of 2, (c) after applying boundary damping forces to the stretched M' .

5. Results

We use a GPU implementation of semi-implicit Euler integration for running the physical relaxation on high-resolution meshes. For simplicity, constant vertex masses of $m = 1$ are used. Besides the edges of M' , our spring system also adopts cross springs over winged triangle pairs [LZL*05]. In all our examples, we use an initial stretch factor of $s = 2.0$, a spring stiffness of $k = 0.5$, and interior and boundary damping coefficients as noted in Section 4. To support reasonable interpretation of the results by the domain experts, we provide a visualization of the amount of distortion together with the final flattened images [SvLB10, WAN02]. Local residual stress is visualized using a heat map overlay depicting the length-normalized root-mean-square distortion per vertex:

$$RMSE(i) = \sqrt{\sum_{j \in \mathcal{N}_i} (\|x_i - x_j\| - r_{ij})^2 / \sum_{j \in \mathcal{N}_i} r_{ij}} \quad (3)$$

To evaluate our method, we created true-to-scale high-resolution 3d models of three different types of ancient vessels with strongly curved surface profiles: an Attic red-figured hydria (c. 470 BC), containing a frieze of the mythological farewell scene of Triptolemos and Kore (2.3M vertices, Fig. 1); an amphora (470–460 BC) depicting opposed-sided images of Nike (515K vertices, Fig. 3) and a young man (303K vertices, Fig. 2); and a Corinthian black-figured alabastron showing a Typhon (600–590 BC), whose motif is wrapped around the entire surface (Fig. 4). For the alabastron, the entire figural frieze (2.6M vertices) was unrolled and used for our elastic flattening. For the hydria and the amphora, only cutouts of the sections containing the friezes were used, which conventional trace-offs would be restricted to as well. The initial cuts have been chosen to be conservatory and as symmetric as possible.

Figure 1 compares currently used conical and spherical rollouts to our elastically flattened result. As seen at the highlighted head of Triptolemos and Kore's torch, our method much better preserves local proportions and straight lines in important regions, trading them



Figure 3: (a) Initial projection of a Nike frieze cutout. (b) Elastic relaxation. The right side depicts residual stresses of both versions.

for a subtle bending of the less important pedestal ornament via a global distribution of stretch energy. In contrast, Fig. 3a uses an orthogonal projection of the Nike frieze using a tilted angle which manually balances the initial distortion between its head close to the pole and the rest of the surface. After relaxation, Fig. 3b shows a clearly minimized overall distortion. As expectable, the stress map indicates only minor residual strain energy at the upper pole. Using current rollouts techniques, the problematic region in the Typhon image is the lower area covering the Typhon's tail and swan's legs, which are strongly squeezed due to the conical approximation (Fig. 4). Again, an elastic relaxation manages to appropriately expand this part and produce an improved overview of the painting.

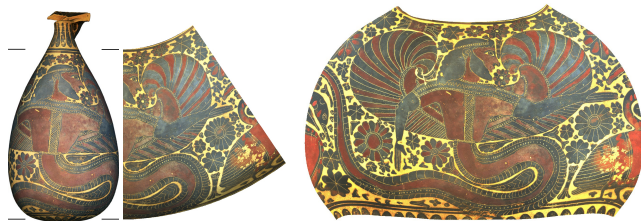


Figure 4: Conic rollout of the alabastron (left) and our elastic relaxation result (right).

6. Conclusion and Future Work

We presented a physically based method for minimizing distortion in flat rollouts of painted ancient pottery models. Adopting previous techniques relaxing strained mass-spring systems, we propose an efficient physical setup allowing for a robust and controlled convergence via a contraction-directed simulation. In the future, we will investigate methods for finding optimal opening cuts for the rollouts that avoid cuts through important motifs like the swan in Fig. 4. We further want to investigate interactive techniques allowing domain experts to locally manipulate local surface elasticity properties to allow for an importance-driven error distribution.

References

[BKMK10] BECHTOLD S., KRÖMKER S., MARA H., KRATZMÜLLER B.: Rollouts of fine ware pottery using high resolution 3d meshes. In *Proceedings of the 11th International Conference on Virtual Reality, Archaeology and Cultural Heritage* (2010), VAST'10, pp. 79–86. 2

- [CWB11] CHEN W., WEI P., BAO Y.: Surface flattening based on linear-elastic finite element method. 2
- [FH05] FLOATER M. S., HORMANN K.: Surface parameterization: a tutorial and survey. In *Advances in Multiresolution for Geometric Modelling* (Berlin, Heidelberg, 2005), Dodgson N. A., Floater M. S., Sabin M. A., (Eds.), Springer Berlin Heidelberg, pp. 157–186. 2
- [Gra14] GRAEPLER D.: Künstlerhand und kennerauge: Die zuschreibung als archäologisches methodenproblem. In *Töpfer Maler Werkstatt: Zuschreibungen in der griechischen Vasenmalerei und die Organisation antiker Keramikproduktion* (October 2014), Eschbach N., Schmidt S., (Eds.), C.H. Beck, pp. 14–24. 1
- [LZL*05] LI J., ZHANG D., LU G., PENG Y., WEN X., SAKAGUTI Y.: Flattening triangulated surfaces using a mass-spring model. *The International Journal of Advanced Manufacturing Technology* 25, 1 (Jan 2005), 108–117. 2, 3
- [LZX*08] LIU L., ZHANG L., XU Y., GOTSMAN C., GORTLER S. J.: A local/global approach to mesh parameterization. In *Proceedings of the Symposium on Geometry Processing* (2008), SGP'08, pp. 1495–1504. 2
- [Mac04] MACEACHREN A. M.: *How Maps Work - Representation, Visualization, and Design*. Guilford Press, 2004. 2
- [MCC99] The flattening of triangulated surfaces incorporating darts and gussets. *Computer-Aided Design* 31, 4 (1999), 249 – 260. 2
- [MP13] MARA H., PORTL J.: Acquisition and documentation of vessels using high-resolution 3d-scanners. 25–40. 2
- [Ric36] RICHTER G. M.: *Red-Figured Athenian Vases in the Metropolitan Museum of Art, Vol 1 & 2*. Metropolitan Museum of Art, 1936. 1
- [Sch] SCHMIDT S.: Zuschreibungen in der griechischen vasenmalerei und die organisation antiker keramikproduktion. geschichte und perspektiven der forschung. In *Töpfer Maler Werkstatt*, pp. 7–13. 1
- [Sch99] SCHREIBER T.: *Athenian vase construction: a potter's analysis*. Getty Publications, 1999. 2
- [SdS01] SHEFFER A., DE STURLER E.: Parameterization of faceted surfaces for meshing using angle-based flattening. *Engineering with Computers* 17, 3 (Oct 2001), 326–337. 2
- [SLMBy05] SHEFFER A., LEVY B., MOGILNITSKY M., BOGOM YAKOV A.: Abf++: Fast and robust angle based flattening. *ACM Transactions on Graphics* (Apr 2005). 2
- [SPR06] SHEFFER A., PRAUN E., ROSE K.: Mesh parameterization methods and their applications. *Found. Trends. Comput. Graph. Vis.* 2, 2 (Jan. 2006), 105–171. 2
- [SvLB10] SCHRECK T., VON LANDESBERGER T., BREMM S.: Techniques for precision-based visual analysis of projected data. *Information Visualization* 9, 3 (2010), 181–193. 3
- [VW08] VAN WIJK J. J.: Unfolding the earth: myriahedral projections. *The Cartographic Journal* 45, 1 (2008), 32–42. 2
- [Wal08] WALTER C.: *Towards a More 'Scientific' Archaeological Tool: The Accurate Drawing of Greek Vases between the End of the Nineteenth and the First Half of the Twentieth Centuries*, ned - new edition, 1 ed. Berghahn Books, 2008, pp. 179–190. 1
- [WAN02] Surface flattening based on energy model. *Computer-Aided Design* 34, 11 (2002), 823 – 833. 2, 3
- [WAN05] Freeform surface flattening based on fitting a woven mesh model. *Computer-Aided Design* 37, 8 (2005), 799 – 814. CAD '04 Special Issue: Modelling and Geometry Representations for CAD. 2
- [YYZ*18] YI B., YANG Y., ZHENG R., LI X., YI M.: Triangulated surface flattening based on the physical shell model. *Journal of Mechanical Science and Technology* 32, 5 (May 2018), 2163–2171. 2
- [ZHO06] A physically based method for triangulated surface flattening. *Computer-Aided Design* 38, 10 (2006), 1062 – 1073. 2
- [ZLS07] ZAYER R., LEVY B., SEIDEL H.-P.: Linear angle based parameterization. In *ACM/EG Symposium on Geometry Processing conference proceedings* (2007). 2